Gravitation and Geodesy with Inertial Sensors, from Ground to Space

Pierre Touboul, G. Métris, H. Sélig, Olivier Le Traon, Alexandre Bresson, Nassim Zahzam, Bruno Christophe, Manuel Rodrigues

P. Touboul
(ONERA)

G. Métris
(Geoazur – CNRS/UMR)

H. Sélig
(ZARM Space Science Department
University of Bremen)

**O. Le Traon, A. Bresson,
N. Zahzam, B. Christophe,
M. Rodrigues**
(ONERA)

E-mail: pierre.touboul@onera.fr

DOI: 10.12762/2016.AL12-11

Gravitation and Geodesy with Inertial Sensors, from Ground to Space

Since the years 2000, three space missions, CHAMP, GRACE, and GOCE, have led us to consider the Earth's gravitational field and its measurement in a new light, using dedicated sensors and adequate data processing, revealing the changes in the Earth's field as the true signal rather than the disturbing terms in addition to the geostatic reference field. Besides the possibilities offered by new technologies for the development of inertial sensors, a space environment of course involves special constraints, but also allows the possibility of a specific optimization of the concepts and techniques well suited for microgravity conditions. We will analyze and compare with others the interest in the electrostatic configuration of the instruments used in the main payload of these missions, and we will consider the recent MICROSCOPE mission, which takes advantage of the same mission configuration as a gradiometry mission to test the universality of free fall whatever the mass composition. A few days after launching the satellite in April 2016, we will show how we intend to validate the future result, the existence or not of a violation signal of the equivalence principle, taking into account the laboratory tests, where available, and the in-flight demonstrated performance during the calibration phases and the scientific measurements. With regard to ground measurements, either fixed or mobile, or under marine or aircraft conditions, we will demonstrate the complementary interest of the atomic interferometer. Finally, we will briefly discuss the future envisaged for these technologies, like that already implemented in the Lisa-Pathfinder mission without a gold wire for the electrical control of the charges of the mass, and these types of mission.

Introduction

We have passed the century anniversary of General Relativity [1], which remains the geometrical foundation of gravity, after thirty years of non-conclusive efforts with String theories and others, like quantum loop gravity: no consistent quantum theory of gravity exists as yet. Attempts to go beyond the Standard Model recently confirmed by CERN with the detection of the Higgs boson [2] and to unify the gravitational interaction with the three other interactions, electromagnetic, weak and strong, have mostly led to the discovery of new particles and forces. Accurate cosmological observations have led to the discovery of the existence of dark energy and dark matter for 95 % of our Universe, while gravity wave observatories are now operating after the first modeled signal of two merging black holes [3].

This context motivates the quest for new observations and for laboratory or space experiments to test gravity and in particular to test the Equivalence Principle, which is the basis of the theory of general relativity. In order to perform such an Equivalence Principle test in orbit, we have optimized the instrument configuration of the space accelerometers that were integrated on board three successive geodesy space missions launched during the last decade [4], [5], [6].

All of these instruments take advantage of the space environment. Thus, they have been configured differently from more conventional inertial sensors used for navigation, and are now based on MEMS (Micro-Electro-Mechanical Systems) technologies for size and cost reduction, while preserving high performance for some. Some are based on the old spring-mass concept, but surpass the nominal limits because of their high-resolution capacitive position sensors, their servo-loops and their electrostatic levitation of a specific solid mass. They nevertheless require dedicated ground and flight calibration with specific facilities.

In-orbit performance of several tens of pico-g has been demonstrated, while the detection of the femto-g signal is expected with the MICROSCOPE mission, launched on April 25 this year, in the case of a well-defined sine at a very low frequency of about 10^{-3}Hz. The operation of an inertial sensor, whatever the technology and the concept are, considers the proof-mass in a geodesic motion, which is subject not only to the gravitational field but also to the acceleration field and to any accurately measured force. Thus, in free fall, the inertial sensor output is nullified, as the difference of the gravitational field and the acceleration field (assuming the weak equivalence principle); when the inertial sensor is fixed to a moving body, the sensor output is the difference of the acceleration of the body and the gravitational field. Thus, it is possible to deduce from the provided data, information on either the inertial acceleration or the gravitational field, and on the difference in the MICROSCOPE specific experiment. Atomic wave interferometry involves, in the same way, both fields and will in the future be an interesting new complementary technology. The Lisa-Pathfinder space mission is also the technological way to test new technologies and, in particular, the control of the test-mass charge without any contact [99], [100].

This paper offers an overview of the driving parameters and characteristics of these instruments, the mission concepts and some specific needed procedures, to compare them with other technologies and similar applications, and to analyze their perspective with regard to future space missions or airborne campaigns for the understanding and mapping of gravity.

Inertial sensors

Over this last century, inertial sensors have experienced continuous improvement, from the early guidance and navigation systems and the "famous" German V2 ballistic missile of World War II, followed by the Cold War and the Space Race through the emblematic Apollo program and the first humans on the Moon with Apollo 11 on July 20, 1969, to the recent period with both the arrival of the Global Positioning System and micro/nanotechnologies, enabling today precise navigation with a simple smartphone.

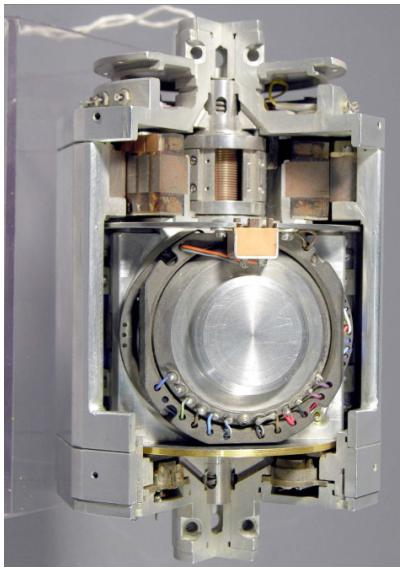

Figure 1 – 25 Piga Accelerometer for the Titan II Intercontinental Ballistic Missile – *Courtesy of AC Spark Plug Division, General Motors Corporation*

The "Pendulous Integrating Gyroscope Accelerometer", PIGA, [7] [8] invented by F.K. Mueller for the V2 missile guidance, remains today the most accurate high dynamic range accelerometer (~50 g range, stability and resolution on the order of 0.1 μg), but is also very complex, bulky (0.5 liter volume and a weight of 3.5 kg for most integrated PIGA) and very expensive to manufacture (Figure 1). The PIGA is based on the conversion of an acceleration input into a gyroscopic torque, induced by a gyroscope in a pendulous configuration. The whole pendulum is mounted into a housing, and the whole pendulum is able to rotate in order to compensate for the gyroscopic torque induced by the acceleration. The rotation rate of the housing is thus proportional to the acceleration input and the rotation angle directly gives the velocity, which is very interesting for precise ballistic systems. However, PIGA accelerometers are sensitive to rotation along the input acceleration axis and need a gimbaled inertial platform, which further complicates the inertial system.

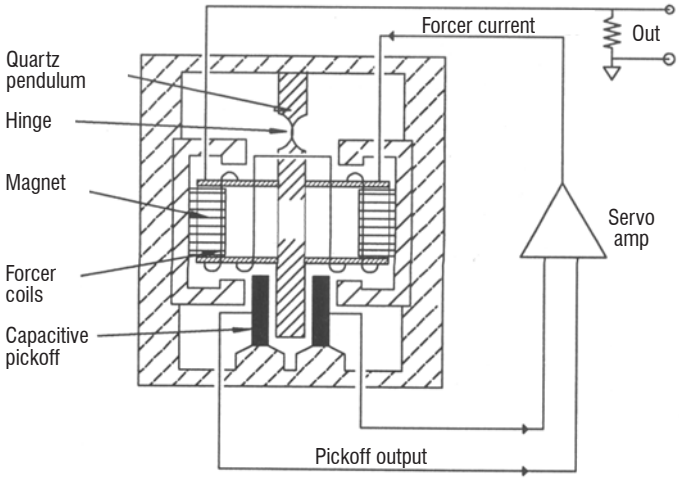

(a)

(b)

Figure 2 – (a) closed loop spring mass accelerometer proposed by Sundstrand (now Honeywell), (b) the famous one-inch diameter inertial grade Q-flex QA3000 accelerometer – *Courtesy of Honeywell*

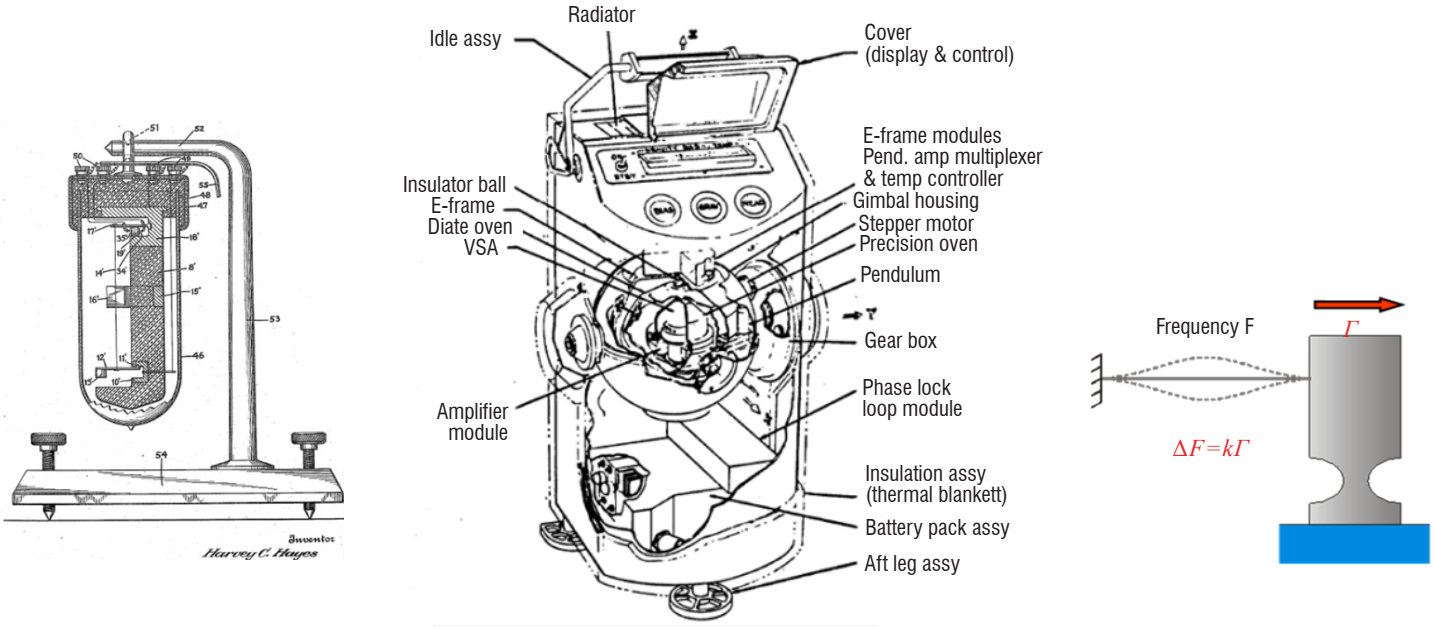

Figure 3 – (a) first vibrating string gravimeter proposed by H. C. Hayes in 1928, (b) lunar VSA gravimeter proposed by the Charles Stark Draper Laboratory for the Apollo 17 mission, (c) vibrating beam accelerometer, the string is changed by a beam in bending mode

The spring mass concept is the conventional configuration of an accelerometer and has known major improvements following the "strap-down" inertial navigation proposed in the early 1970's (i.e., the inertial components are directly mounted on the vehicle, without a gimbaled inertial platform). Figure 2 shows the nominal configuration, either in open or closed loop, and the "Q-flex" accelerometer proposed in the 1990's by Sundstrand [9] (now Honeywell) remains a reference for wide range inertial navigation grade accelerometers. Thanks to its magnetic feedback and to its particularly high-stability quartz hinge, it reaches a high measurement range of ± 60 g, while exhibiting a one year bias stability (all errors combined) better than 40 μg, a scale factor repeatability better than 80 ppm and an intrinsic noise of a few $\mu g/\sqrt{Hz}$.

Another very surprising kind of spring mass accelerometer is the Vibrating Beam Accelerometer (VBA). Vibrating Beam Accelerometers (VBAs) are based on the change in the resonance frequency of a vibrating beam when subjected to acceleration (Figure 3a). The idea of the direct conversion of the acceleration in the change of a resonator frequency is not new and was first proposed in 1928 [10]. At that time, the resonator was a metallic string, excited to its resonance frequency by electromagnetic forces, whence the name of Vibrating String Accelerometer (VSA). A basic limitation of VSA was its inherent poor bias stability (frequency stability under zero acceleration), mainly due to the necessary pre-tension of the string and also to the low quality factor of the string. However, it must be noticed that, within the context of the Apollo program in the 1970's, lunar gravity was successfully measured with an accuracy of 1 m-gal (10^{-5} m/s^2) thanks to a Vibrating String Accelerometer, including a reversal system in order to reject the bias [11].

A first major evolution of vibrating accelerometers was achieved by changing the string for a vibrating beam in flexure mode [12]: thanks to its compression stiffness, a vibrating beam doesn't require pre-tension, enabling the improvement of the bias stability. The beam geometry has very often been a research subject in order to reduce the impact of its mounting on the accelerometer structure and to preserve the quality factor of the beam (generally made of quartz crystal). Various beam geometries have been proposed: a simple beam held at its nodal lines [13] [14] [15], a simple beam with decoupling systems on its ends [16] [17] [18] [19], optimized double tuning forks [20] or a triple-beam resonator [21]. Industrial developments of vibrating beam accelerometers (VBA) have been undertaken, leading at the end of the 80s to commercial products, such as the well-known RBA 500 [22], which is still in production today [23].

At the end of the 1980's, riding the waves of the Micro Electro Mechanical System (MEMS) revolution, heavily used by the silicon industry [24], monolithic VBA structures – i.e., the whole accelerometer structure, including not only the proof mass but also the hinges and the beam resonator – made of the same material (generally quartz or silicon crystals) emerged [25] [26] [27] [28]. A monolithic accelerometer structure presents a lot of advantages: reduction of pieces and adjustment, matching of the thermal behavior, elimination of the delicate resonator mounting onto the accelerometer structure, and compatibility with collective micromachining techniques. Thus, all of these points are well suited to optimize the accelerometer accuracy and miniaturization, with a potential of a low manufacturing cost. Quartz and silicon VBA have been developed. The first of these takes advantage of the intrinsic piezoelectricity of quartz crystals, which enables an easy and accurate excitation and detection of the vibrating beam. The second benefits from the amazing developments in the semiconductor and microelectronics industry. Examples of VBAs that have been developed, mainly for military applications, leading or not to industrial products, are given in [29] [30] [31] for quartz devices and in [32] [33] [34] [35], [36] [37] for silicon devices. ONERA was one of the first laboratories to propose a monolithic configuration for the VBA [27] [33], and has developed the VIA accelerometer, which has now been transferred to

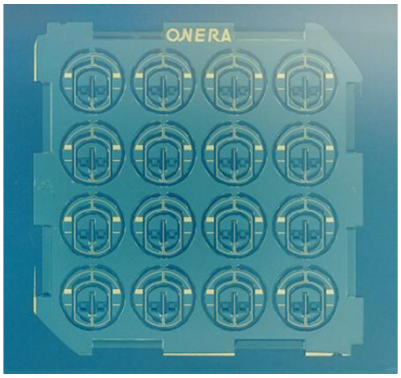

Quartz Wafer (1.5" x 1.5")

VIA Accelerometer

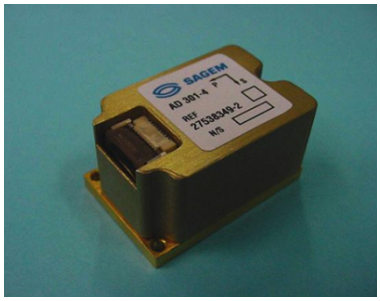

AD301 SAGEM
Quartz VBA

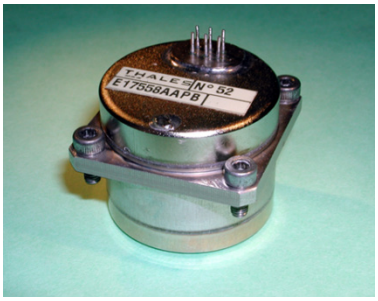

A100 THALES
Quartz VBA

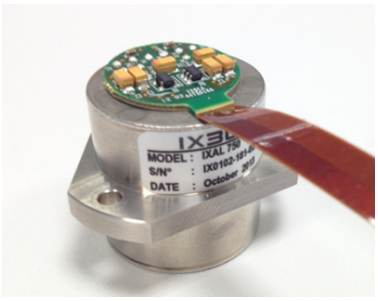

IXAL750 IXBlue
Quartz VBA

Figure 4 – Quartz Vibrating Beam Accelerometer developed at ONERA. (a) quartz wafer with 16 VIA accelerometers, (b) detail of the monolithic VIA accelerometer mounted on a base, (c) Vibrating Beam Accelerometers based on the VIA concept and produced by the companies SAGEM, THALES and IXblue.

industry [39] [40] [41] (Figure 4). The main originality of the VIA concept lies in the use of a simple beam as a vibrating resonator and of a monolithic insulating system around the beam and the proof mass, allowing a very efficient insulation of the beam vibration. This insulating system preserves the high quality factor of the quartz beam, as well as any thermal stresses due to the mounting of the sensitive monolithic quartz element onto its base, which are two necessary conditions for achieving high bias stability. The VIA Quartz MEMS accelerometer is an excellent tactical grade accelerometer with a measurement range of 100 g, an excellent scale factor stability better than 10 ppm, a bias stability (all errors combined) better than 300 μg, a scale factor stability better than 10 ppm and a resolution of 1 μg @ 10s (until now, no equivalent MEMS device has been produced in the world).

New Quartz MEMS VBAs are under development at ONERA. They are aimed at reaching the navigation and strategic grades, taking advantage on the one hand of the important improvements in quartz microtechnology and on the other hand of innovative concepts [42] [43], as well as progress in analogic/digital electronics able to perfectly control the oscillator circuit phase. Figure 5 shows two of the VBAs being studied: the navigation grade DIVA accelerometer (Differential Inertial Vibrating Accelerometer) with a measurement range of 50 g, a bias stability better than 50 μg (all errors combined) and a noise better than 1 μg @ 10s, and the high-resolution AVAS [44] with a noise of 50 nano- g @ 10s, a bias stability better than 1 μg and a measurement range of 10 g.

Other interesting configurations are also presently being studied at the micrometric scale, including original detection schemes such as optical [45], or electron tunneling effect schemes [46], with an excellent resolution of 20 nano-g, which is near the thermomechanical noise limit due to the small proof mass (in the milligram range) of

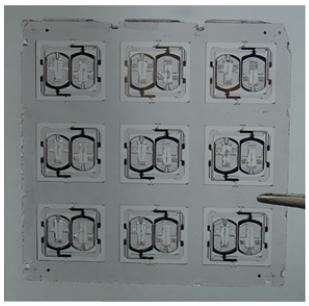

DIVA VBA

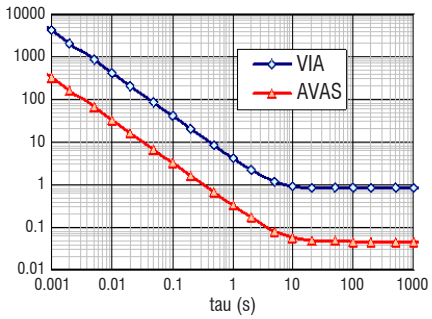

AVAS VBA

Figure 5 – Quartz MEMS Vibrating Beam Accelerometer under development at ONERA. Left: DIVA (Differential Inertial Vibrating Accelerometer) navigation grade VBA. Right: AVAS high-resolution VBA with a 50 nano-g resolution @10s.

this MEMS device. "On Earth" acceleration measurements are indeed subject to a compromise between measurement range and resolution. Fortunately, Space is another Universe (with other constraints).

Space environment and dedicated sensors

Space can be regarded as a constraint when developing an instrument, considering the importance of demonstrating the instrument reliability, the traceability of all procedures (production, maintenance, tests, etc.), the robustness to the radiation environment, and the resistance to launch vibrations and thermal vacuum. On the other hand, it can also be seen as an opportunity: one space mission can consider a global coverage of the Earth for a limited time and without geographical or political access difficulties. It can take advantage of the fine space environment provided by the satellite: magnetic, with shielding from the Earth's or the spacecraft's residual field; electrical, with shielding also; thermal, with rather well-defined external conditions and internal power sources; vibrations and gravitational fields, thanks to the satellite design and stiffness, without moving or rotating masses; the satellite can take advantage of a drag compensation system when the orbit of the satellite is too low to neglect the effects of the atmospheric drag and its fluctuations [47], or when specific requirements must be met when considering the maximum level of acceleration that the instrument is subjected to.

Micro-gravity operation can also been seen as an opportunity, when weak accelerations have to be detected or measured. In the case of an inertial sensor, it is the possibility of neglecting the normal gravity level, as large as 9.81 ms^{-2}, when considering the full scale range (FSR) of your sensor, thereby increasing its resolution, which is always a limitation for part of the FSR. As a rule of thumb, the atmospheric drag of a satellite equals its radiation pressure at around 700 km, like the altitude of the MICROSCOPE satellite [48], and reaches several 10^{-7} ms^{-2} at the altitude of the GRACE and CHAMP satellites, i.e., 450 km to 500 km [49], [50], and 10^{-5} ms^{-2} at very low altitude, like 270 km in the case of the GOCE satellite [51]. Thus, the FSR of the space inertial sensor can be reduced by a factor 10^6 with respect to those of ground, missile or aircraft sensors, allowing other technologies.

The resolution of an inertial sensor based on the spring-mass concept depends dramatically on the stiffness of the spring and the resolution of the position sensor that will detect the mass motion with respect to its fixing point (see Figure 6). While $N_x(f)$ is the power spectrum of the position detector noise, $N_\Gamma(f)$, the induced power

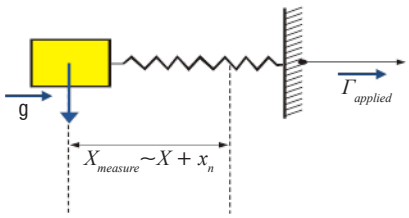

Figure 6 – Inertial sensor mass-spring concept: the acceleration of the accelerometer structure applied in the direction of the spring is measured through the displacement of the inertial mass, as well as the gravitational field applied to the proof-mass when it is in the spring axis

spectrum of the inertial sensor output is simply expressed by taking also into account the Nyquist noise, which is especially important at low frequencies, [52], [53] induced by the spring damping:

$$N_\Gamma(f) = N_x(f).16.\pi^4.\left(k/m + f^2\right)^2 + 1/m^2.\left(4.k_B.T.k/\left(2\pi.f.Q(f,T)\right)\right)$$

where k and Q, define the stiffness and the damping (through its quality factor) of the spring respectively, T is the temperature of the device, k_B is Boltzmann's constant, and f is the frequency of interest. In order to exhibit a very low acceleration noise, N_x and k must be limited. However, the frequency response of the spring-mass device depends mainly on the value of k when the mass is passive and not servo-controlled.

Let s be the Laplace variable expressing the derivation, and $\left(X(f) + xn(f)\right)$ the measurement of the proof-mass position (see Figure 6) from which the acceleration is deduced and that is servo-controlled to null; the frequency response of the sensor can then be expressed by:

$$\hat{\Gamma} \approx -\frac{k}{m}.\left(X(f) + x_n(f)\right)$$

when the mass is passive (in open loop operation) and

$$\hat{\Gamma} \approx -\frac{(2.\pi.f_c)^2}{(2.\pi.f_c)^2 + k/m + s^2}.\left(\Gamma(f) + \left(s^2 + k/m\right).x_n\right)$$

when the mass is servo-controlled (where f_c is the cut-off frequency of the control loop bandwidth simply defining the loop gain; the corrector may be more complex, but here it is only represented by this gain).

Thus, the sensor noise in the last case can be reduced by nullifying the stiffness, while the sensor frequency bandwidth is preserved by the loop control bandwidth. It is also important to point out that the damping provided by the corrector of the electrostatic loop (not considered in the above equation for simplicity purposes) is a "cold" damping that is not considered when computing the Nyquist dissipation [54]. In addition, the perturbing accelerations applied directly to the mass (magnetic, electric, thermal and gravitational), which may depend on the geometry of the mass environment, do not fluctuate because of the motionless mass.

Two types of technology have been proposed for mass levitation and its position sensing. One consists of a magnetic superconducting suspension [55], making use of the sensibility of squid devices for the position detector [56], [57] and operating at a cryogenic temperature, mainly at liquid He temperature, 4.2 K, or even lower. The SQUID detects the motion of the mass in front of a superconductive loop through the variation of the induced magnetic flux. The stability of the suspension and the resolution of the SQUID benefits from the low temperature and the superconducting shielding. However, the mass is not servo-controlled and the operation on board a satellite is very complex due to the helium Dewar and the necessary adjustment of the different currents of the loops corresponding to the right position and attitude of the levitated mass. Superconducting accelerometers [58],[59] have been proposed in the past for various space missions, but have never been selected by NASA or ESA, as gavity-gradiometers [60], [61], that can nevertheless benefit of specific SQUID circuits to perform directly the differential measurements of the test-mass positions and accelerations.

The other consists in the electrostatic levitation of the test mass; this is what has been done for the GPB mission [62] gyrometer ball, with the servo control of its position, only three degrees of freedom (translations), while the attitude of the spinning ball is deduced from the London effect. Given that the ball rotates with respect to the cage electrodes, its precise motion is very sensitive to the patch effects on both conductors [63]. When the six degrees of freedom of the cubic proof-mass are servo-controlled, the levitation is only biased by these potentials, which introduce only DC offsets into the inertial sensor outputs. Thus, the patch fluctuations are the only ones to be considered when one is interested by a signal at a frequency that is not at DC.

This is the electrostatic configuration of the CHAMP, GRACE and GOCE accelerometers [64]. The solid metallic proof-mass is surrounded by at least six pairs of electrodes. Each pair of opposite electrodes performs the capacitive measurement of the mass part between the two, and the differences in voltage between the mass and the electrodes are controlled and generate electrostatic pressures that lead to mass forces and torques. The resultant is finely measured to provide the six acceleration outputs (3 linear and 3 angular) of the inertial sensor; the orthogonal faces of the conductive mass define the frame of the six outputs [65].

The drag-free sensor of the current Lisa-Pathfinder space mission [66] is also based on the electrostatic control of a solid mass. In science mode, along the interferometric direction, the mass must follow a geodesic motion without any non-gravitational force and the detection of the gravitational wave comes from the optical interferometer output. Thus, along the interferometer axis, this is different and the acceleration of the mass does not depend on the servo-electrostatic forces, which must be finely measured by the sensor itself when accelerometers are considered. Thus, the configuration can be optimized in a different way, in particular considering only the sensitivity of the capacitive sensing for measurement [67], [68].

Performance of the GOCE mission, GRACE-FO mission and MICROSCOPE mission electrostatic instruments

One of the main challenges in the realization of the space accelerometer is the verification of the performance. Indeed, due to the presence of gravity on the ground, it is not possible to verify this performance through a dedicated test. The strategy for the verification relies on a combination of the mathematical formulation of the impact of each contributor, specific tests for assessing the level of this contributor, and finally flight verification through the post-processing of the flight data.

For each type of mission, the first step to determine the performance of the instrument is to write the measure equation. For the CHAMP, GRACE or GRACE-FO missions, the accelerometer mainly measures the non-gravitational forces (residual drag, solar radiation pressure, etc.) exerted on the spacecraft. For the MICROSCOPE and GOCE missions, the use of several accelerometers inside the spacecraft enables the measurement of the differential acceleration between accelerometers: this measurement enables either the Eötvös parameter (related to the Einstein equivalence principle) or the gravity gradient to be determined. To simplify, we will focus on the first type of missions, the measurement of the non-gravitational acceleration. For the GOCE or MICROSCOPE missions, the accelerometers also measure this acceleration (used for example for the drag compensation), and the difference in acceleration allows just the impact of the common acceleration to be reduced.

In principle, the output of an electrostatic accelerometer, like those developed by ONERA, is the relative acceleration between the proof-mass and the electrode cage, which is applied through the electrostatic forces to maintain the proof-mass at the center of this cage. The cage is servo-controlled and fixed to the spacecraft, so its acceleration is due to the acceleration applied to the center of gravity of the spacecraft and to the inertial acceleration if the accelerometer is not at the center of gravity. The proof-mass is nominally subjected only to the gravitation acceleration at its location. Taking into account parasitic acceleration on the proof-mass and the spacecraft, or deformation of the spacecraft, the acceleration as seen by the accelerometer is expressed by the following equation:

$$\underline{a}_{ACC} = \underline{a}_{NG} - [U]\underline{r} + \left([\dot{\Omega}] + [\Omega^2]\right)\underline{r} + \underline{a}_{para\_SC} + \underline{a}_{para\_acc} + 2[\Omega]\dot{\underline{r}} + \ddot{\underline{r}}$$

Where $\underline{a}_{NG}$ represents the non-gravitational acceleration,

$[U]$ is the gravity gradient tensor,

$\underline{r}$ is the vector between the proof-mass location and the center of gravity, $\dot{\underline{r}}$ and $\ddot{\underline{r}}$ being the velocity and acceleration of this vector in the spacecraft reference frame (therefore representing the deformation of the spacecraft),

$[\dot{\Omega}]$ and $[\Omega^2]$ are the angular rate and acceleration tensors,

$\underline{a}_{para\_SC}$ is the parasitic acceleration due to the spacecraft (e.g., the magnetic perturbation),

$\underline{a}_{para\_acc}$ apara_acc is the parasitic acceleration due to the instrument (e.g., the radiometric effect).

The 2 first terms generally represent the signal that we want to measure (for GRACE or GRACE-FO, we want to measure the residual drag, for GOCE we want to measure the gravity gradient tensor). The other terms represent errors to be minimized or corrected.

Beyond these terms, it is also necessary to take into account the fact that the acceleration seen by the accelerometer is not perfectly measured, due to the imperfect scale factor ($[dK]$), the instrument noise (n) or bias (b), the non-linearity ($[K2]$) or the imperfect alignment or the coupling between the axes ($[R+S]$), leading to additional sources of errors:

$$\underline{a}_{meas} = \underline{a}_{ACC} + [dK]\underline{a}_{ACC} + \underline{n} + \underline{b} + [K2]\underline{a}^2_{ACC} + [R+S]\underline{a}_{ACC}$$

Often, the performance of an accelerometer is defined by its noise in a frequency-amplitude space. Most of the engineering design activity consists in first reducing, and second optimizing and tuning the noise of the various contributors with respect to the target bandwidth and the required level specification. The noise from the electronics is precisely measured on the ground and converted into acceleration. The parasitic noise contributions are deduced from a specific test ([69], [70]).

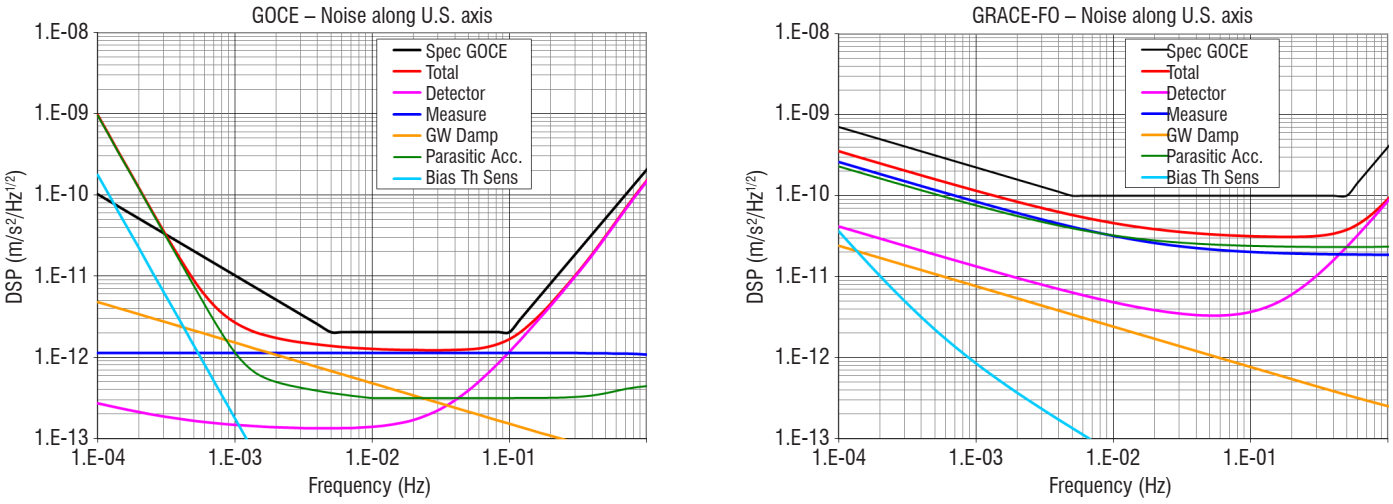

Figure 7 – Noise performance of the GOCE accelerometer (a) and GRACE-FO accelerometer (b) along their ultra-sensitive axis

The result is shown in Figure 7, for the GOCE [71] and GRACE-FO [72] accelerometers, at the same scale for comparison, where only the main contributors have been selected:

- The detector noise (pink). This is basically due to the electronic noise in the detector circuit; the control loop induces a detector noise increase with frequency.
- The wire damping (orange): a thin gold or platinum wire is used to impose the mass electrical potential, whatever the space radiation. The wire stiffness and damping is minimized by the use of a 5 μm diameter gold wire on GOCE and a 7 μm diameter platinum wire on GRACE-FO; the effect of the wire damping in the control loop produces a noise level limit that fortunately remains far below that required.
- The measurement readout and digitalization noise (dark blue). Usually, in digital circuits the quantification step of the measurement device is designed well below the noise level of the instrument and is not a limiting point. The present situation is the best trade-off between the range needs and the measurement noise.
- The thermal sensitivity of the bias (light blue). Despite the accelerometer thermal control, the temperature variation leads to the variation of the electronic bias at low frequencies. In the case of GOCE, the gradiometer manufacturer announced a great increase in the temperature stability at very low frequency, which was pessimistic.
- The parasitic acceleration inside the accelerometer core (green). The main contributors are the thermal sensitivity of the radiometer effect, due to the difference of temperature between the faces of the proof-mass, and the patch effect due to the electrode and proof-mass surface states.

Since the performance is not achievable on the ground, flight post-processing enables the performance prediction to be confirmed. When only one accelerometer is present (like in the case of the GRACE mission), the in-flight verification will be done during a quiet period and will suffer from the low frequency drag. Nevertheless, the accelerometer performance has been verified for GRACE ([73]). In the case of GOCE, the combination of several accelerometer outputs eliminates the common mode (the residual drag) and yields information on the intrinsic performance. It has also been possible with GOCE to verify the electronic noise or internal stiffness in orbit, thanks to the versatility of the digital loop ([74]).

Validation of the inertial sensor performance

During the development of the sensor, three types of tests are performed to validate the expected performance. On the one hand, the geometries of the mechanical parts of the sensor, and in particular the test-mass, are finely controlled after their machining and throughout their integration in a clean room (size accuracy: down to the micron, parallelism, orthogonality, as well as the material properties: homogeneity of density, magnetic susceptibility, conductivity, cleanliness, etc.). On the other hand, the performance of the electronic units [81] is verified (sensitivity, bandwidth, linearity, noise spectrum, and thermal sensitivity) leading, for instance for the MICROSCOPE sensor configuration, to the following flight model results:

- Capacitive position sensors

Axis	Internal Mass (1.4 kg)	External Mass (0.4kg)
X	2 μVHz$^{-1/2}$ = 4 10^{-11} mHz$^{-1/2}$	6 μVHz$^{-1/2}$ = 2.5 10^{-11} mHz$^{-1/2}$
Y, Z	6 μVHz$^{-1/2}$ = 2.5 10^{-11} mHz$^{-1/2}$	3 μVHz$^{-1/2}$ = 1 10^{-11} mHz$^{-1/2}$

- Electrostatic actuators (electric potentials on electrodes)

Axis	Internal Mass	External Mass
X	1.1 μVHz$^{-1/2}$ = 20 10^{-15} NHz$^{-1/2}$	1.6 μVHz$^{-1/2}$ = 52 10^{-15} NHz$^{-1/2}$
Y, Z	2.3 μVHz$^{-1/2}$ = 160 10^{-15} NHz$^{-1/2}$	2.3 μVHz$^{-1/2}$ = 710 10^{-15} NHz$^{-1/2}$

In addition, the perturbation forces considered in the established error budget [80] must be validated for each instrument: gas damping, radiometer effects, radiation pressure, magnetic susceptibility,

electrostatic patch effects, and damping and stiffness of the thin gold wire used to control the mass electrical potential [82], [83], etc. However, this is not the integrated flight model test.

Inertial sensors for space missions like GRACE [5], GOCE [6] and MICROSCOPE are designed and constructed for operation in a zero-g environment. It is a matter of fact that these sensors and their performance cannot be tested under ordinary laboratory conditions at 1g. In principle, there are various solutions to overcome this general problem: (i) Electrostatic levitation of the test mass in order to enable sensor tests in the horizontal plane, (ii) mechanical levitation of the test mass with a wire and, finally (iii), free-fall tests of the sensors to allow sensor tests in all degrees of freedom at the same time.

The first possibility has been considered in the development of the first mentioned instruments. The proof-mass is levitated in a specific configuration along the vertical axis, while the two other axes are tested near the horizontal plane. The laboratory levitation of the mass along the vertical direction requires the smallest gap between the mass and the electrodes, 30 μm instead of 300 μm in the case of the GOCE accelerometer, reducing the resolution of the sensor in space along this axis. On the ground, the voltage applied on the electrodes is also increased due to the presence of normal gravity and can reach levels greater than 1000 V. Furthermore, the sensor must be tested, mounted on an anti-seismic platform, in order to eliminate horizontal disturbances and to maintain the instrument references with respect to the vertical direction. This approach is very interesting when the ground requirements do not interfere with the space performance, because the duration of the tests is not a constraint.

The second possibility has been considered in the development of the LISA-Pathfinder drag-free sensors [75]. However, it takes a huge effort to mimic the configuration of the sensor considered and to measure the torque on the torsion pendulum wire, which represents the phenomenon to be tested. Improvements to the facility are continuously being considered [76], in order to better model the sensor behavior, but the flight models are not actually tested.

This is not the case with the last possibility, which in particular uses the ZARM facility. The drop tower at ZARM allows free fall tests with a zero-g period of between 4.7 and 9.3 seconds, depending on the operation mode of the facility (normal drop mode or catapult mode) [77]. In both modes, a drop capsule with its payload undergoes nearly perfect zero-g conditions inside an evacuated drop tube. For each drop test, the tube must be evacuated by means of high power vacuum pumps. At the end of the free fall phase the capsule is captured by a deceleration chamber filled with small polystyrene balls. For the recovery of the capsule, the drop tube has to be flooded with dried air. The number of drops is limited to three per day. The free fall duration is limited by the height of the drop tube and the corresponding free fall height (110 m for the drop tower in Bremen). Although the best zero-g quality is rather good ($\sim 10^{-6}$g), residual accelerations act on the capsule and the payload. The aerodynamic drag due to the residual air pressure of 10 Pa inside the evacuated drop tube generates acceleration in the opposite direction to that of the capsule velocity vector. The corresponding maximum acceleration is around 10^{-5}g. The second residual acceleration is the centrifugal acceleration due to the residual capsule spin rates. Although these rates are rather small, the payload is mounted near the capsule center of mass, in order to minimize the centrifugal acceleration level. Finally, a certain level of vibrations is induced by the release of the capsule in normal mode or by the initial capsule acceleration in catapult mode. In order to reduce the vibration acting on the payload, a passive damping system is used, which has been tested and optimized in a number of drop tests with a SuperStar sensor provided by ONERA.

The best possible zero-g quality is achieved by using a free flyer platform inside the drop capsule. Due to technical reasons, this option is only available in the normal drop mode. The free flyer is released shortly after the capsule release and captured before impact by a pneumatic system. This technique is interesting, especially for experiments that demand a very high zero-g quality. The zero-g quality is improved by 1-2 orders of magnitude compared to the normal drop capsule. Many drop tests have been carried out for the MICROSCOPE sensor validation using the free flyer technique. The drawback of the free flyer is the relatively short zero-g duration of around 4 seconds, which is insufficient for testing all sensor parameters. Therefore, the final payload tests for MICROSCOPE have been performed in catapult mode. The main advantage of the catapult mode is the long zero-g duration of 9.3 seconds. Another advantage is the possibility of measuring the sensor bias of an accelerometer directly at the highest point of the capsule trajectory [78]. At this point, the capsule velocity is zero and therefore the residual acceleration induced by the drag also vanishes. The time when the capsule reaches the highest point of the trajectory can be calculated very precisely.

The ZARM drop tower team has been cooperating with ONERA for many years, especially in the area of free fall tests of inertial sensors for space missions. The correct zero-g-operation has been demonstrated for the GRACE and GOCE sensors, and finally for the MICROSCOPE

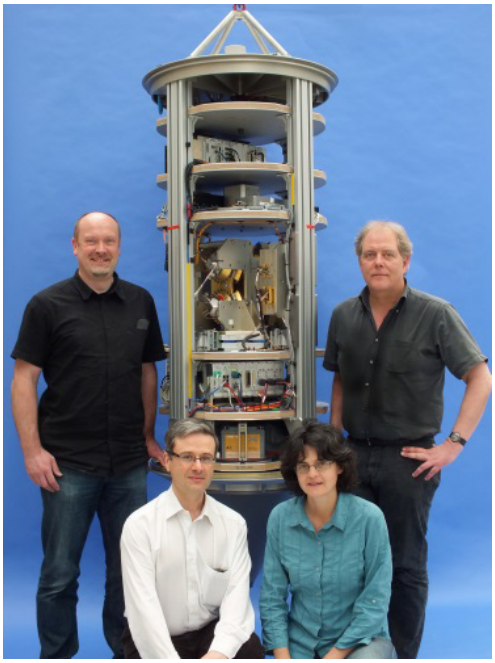

Figure 8 – Catapult capsule for the MICROSCOPE free fall tests at the ZARM drop tower in Bremen. The MICROSCOPE sensor unit is installed close to the center of mass of the capsule. The various platforms carry a computer system, batteries and radio link systems for communication with the control room. For the free fall tests inside an evacuated drop tube, the setup is covered with a pressure-tight aluminum cylinder, which is not shown in this figure.

sensors. According to the corresponding rules, the sensors have been tested before and after vibration, thermal vacuum and shock tests, in order to demonstrate their proper function in space. The tests of the MICROSCOPE sensors required some effort especially, due to having the highest sensor sensitivity and due to the corresponding demand for a very quiet environment and low disturbance level.

However, free fall tests with a duration of a few seconds cannot replace the complete and precise sensor calibration, which always has to be carried out in special calibration measurement sessions during the mission in space. However at least the proper functioning of space accelerometers in all degrees of freedom can be demonstrated very well with the help of the ZARM drop tower facility. Also, some sensor parameters can be roughly evaluated, such as sensor bias and scale factors.

Mission requirements, MICROSCOPE

In the case of MICROSCOPE, which is aimed at testing the Equivalence Principle (EP) in space with an accuracy of 10^{-15}, the mission requirements are directly derived from the test-mass equation of measure, as described in §4. The main difference with other missions is that we distinguish here the inertial mass m_i from the gravitational mass m_g in the equations.

The inertial mass defines the force of inertia to accelerate a body: $\vec{F} = m_i \vec{\Gamma}$.

The gravitational mass defines the weight in a gravitational field: $\vec{F} = m_g \vec{\mathrm{g}}$.

For a body in free-fall in a uniform gravitational field g, Newton's laws lead to the acceleration being expressed as $m_i \vec{\Gamma} = m_g \vec{\mathrm{g}}$.

Einstein postulated as a principle in his General Relativity theory [79] that in a uniform gravitational field the acceleration is equal to the gravity. In other words, in an accelerated vehicle far from any gravitational field, the passenger should be able to perform any physics experiment as if he was in a gravitational field. The consequence is, first, that inertial mass and gravitational mass are equal and second that all bodies in free fall follow the same trajectory regardless of their mass or composition.

In the case of two perfectly concentric bodies in free-fall, the difference in the acceleration felt by the two bodies is:

$\overrightarrow{\Gamma_1} - \overrightarrow{\Gamma_2} = \left(\frac{m_{1g}}{m_{1i}} - \frac{m_{2g}}{m_{2i}} \right) \vec{\mathrm{g}}$ as, since the two bodies are subjected to the same gravitational field $\delta = \frac{2\left(\frac{m_{1g}}{m_{1i}} - \frac{m_{2g}}{m_{2i}} \right)}{\left(\frac{m_{1g}}{m_{1i}} + \frac{m_{2g}}{m_{2i}} \right)}$ is commonly defined as the Eötvös parameter and expresses the deviation from the Equivalence Principle. In a uniform gravitational field, the Eötvös parameter is calculated with the ratio between the differential acceleration and the mean acceleration of the 2 bodies:

$$\frac{\overrightarrow{\Gamma_1} - \overrightarrow{\Gamma_2}}{\left(\overrightarrow{\Gamma_1} + \overrightarrow{\Gamma_2} \right) / 2}$$

Performing the EP test at 10^{-15} accuracy involves measuring and interpreting a difference in acceleration of at least 10^{-15}g, and the previous Eötvös parameter is computed for the two materials with 10^{-15} accuracy.

Actually, to perform the test, two different materials are used: a Platinum alloy (PtRH10: 10% of Rhodium) versus a Titanium alloy (TA6V: 6%Al + 4%V).

Testing the universality of free-fall in orbit, around the Earth, should be an ideal test if one is able to perfectly manage the initial conditions of the free-fall. In order to be more accurate, the free-fall of the test-masses is controlled by electrostatic forces and the test-masses are kept relatively motionless with respect to the surrounding control electrodes. The trajectory is maintained in the same way, and is identical for the two test-masses and identical to the drag-free satellite orbit, thanks to the drag compensation system; and if they are accelerated in the same way, Universality is verified, a dissymmetry in the applied acceleration reveals a violation of the Equivalence Principle. The principle of the electrostatic control is exactly the same as that of the electrostatic accelerometers used for the CHAMP, GRACE or GOCE payloads.

The satellite payload is thus composed of two differential accelerometers, each including two cylindrical and concentric test masses. The masses are made of the same material (PtRh10) for the first one, which is dedicated to assessing the accuracy of the EP experiments and the level of systematic disturbance errors. The mass materials are different for the second one. Then, the experimental procedure is based on a double comparison, in order to eliminate systematic errors. The selection of the mass material is a compromise between the instrument accuracy requirements, the theoretical interest and the technological feasibility.

The first step in establishing the requirements was focused on the test-mass shape. The electrostatic forces applied to the test-masses result from voltages applied on the surrounding electrodes. The geometry of the test-masses defines the capacitive environment used as input to the digital servo control of their motion. The volume forces, like gravity, act at the center of gravity G, which is defined for the volume of the mass by: $\int_V \overrightarrow{GP} \wedge \vec{g}(P)\, \rho dV = \vec{0}$.

The gravitational force exerted by a punctual source Ms (like a spacecraft device) at the test mass center of gravity G_0 is given by

$$\int_V \frac{G_0 Ms}{r^3} \rho(\vec{r}) \vec{r} dV$$

Given that each element of the test-mass is not located at the same distance from the punctual disturbing source, the equation becomes of first order: $mg_z(G) \approx \frac{G_0 Ms}{R^2} \left[m + \frac{3}{2R^2} \left(I_{xx} + I_{yy} - 2I_{zz} \right) \right]$, where z is the direction of the source at a distance R (considered much bigger than the dimensions of the test-mass), and I_{kk} is the main moment of inertia of the test-mass.

In order to neglect the first order term, the spacecraft gravitational field and fluctuation effects on the test-mass acceleration measurements, the cylinders have been manufactured so that their moment of inertia is identical around all axes. The cylindrical test mass can then be considered at first order as a sphere from the point of view

of gravity. The equality of all moments has been achieved at 0.1% by considering variations of 10^{-16}m/s^2 of the spacecraft gravity at orbital frequency (which is the modulation frequency of the Earth's gravity g when the spacecraft is inertial pointing and thus the EP frequency).

Thanks to the hypothesis of spherical inertia of the test-mass, the equation of measure is established as follows for two concentric test-masses [80]:

$$\begin{aligned}\vec{\Gamma}_{mes,d} = \underbrace{\vec{b}_{0d}}_{bias} &+ \left(\left[1+\underbrace{dK_{1c}}_{scale}\right]+\underbrace{[\eta_c]}_{coupl.}\right)\cdot\vec{b}_{1d} \\ &+ \left(\left[1+\underbrace{dK_{1c}}_{scale}\right]+\underbrace{[\eta_c]}_{coupl.}+\underbrace{[d\theta_c]}_{align.}\right)\cdot\vec{\Gamma}_{app,d/sat} \\ &+ \left(\left[\underbrace{dK_{1d}}_{scale}\right]+\underbrace{[\eta_d]}_{coupl.}\right)\cdot\vec{b}_{1c} \\ &+ \left(\left[\underbrace{dK_{1d}}_{scale}\right]+\underbrace{[\eta_d]}_{coupl.}+\underbrace{[\theta_d]}_{align.}\right)\cdot\left(\vec{\Gamma}_{app,c/sat}+\frac{\vec{F}ext_{/sat}}{M_{Isat}}+\frac{\vec{F}th_{/sat}}{M_{Isat}}\right) \\ &+ \frac{1}{2}\underbrace{K_{21}}_{quad}\Gamma_{app,1/sat}{}^2-\frac{1}{2}\underbrace{K_{22}}_{quad}\Gamma_{app,2/sat}{}^2+O\left(dK,d\eta,d\theta,K_2\right)^2\end{aligned}$$

The index d represents the differential mode (the difference between the measured or true accelerations or the mismatching of the sensitivities, scale factors, alignments, etc.); on the other hand, the index c corresponds to the common mode (mean value of the acceleration of the two concentric test masses, or of the scale factors, etc.), $\vec{b}$ is the acceleration bias (due to the mechanics or the electronics defects: these can be affected or not by the lack of knowledge of the scale factor K_1 or the couplings η). Θ represents the misalignment of the test-masses. The nonlinear terms or quadratic terms are noted K_2.

The Eötvös parameter is included in the applied acceleration difference:

$$\Gamma_{app,d/sat} = \frac{1}{2}\delta\vec{g}_{/sat}+\frac{1}{2}\left(T_{/sat}-In_{/sat}\right)\cdot\vec{\Delta}_{/sat}-\frac{1}{2}\left(2[\Omega]_{/sat}\dot{\vec{\Delta}}_{/sat}+\ddot{\vec{\Delta}}_{/sat}\right)$$

This equation shows the effect of the miss-centering Δ of the two test-masses, which are supposed to be concentric: it depends on the local gravity gradient T, or the attitude motion of the satellite In (angular acceleration and centrifugal acceleration).

Finally, we have to consider the possible *a posteriori* corrections of the measurement. Indeed, some of the instrument parameters can be evaluated in orbit by specific motions or stimuli of the satellite to enhance the effect of the defect. Once the parameters are calibrated, it is possible to subtract the contribution of the disturbing effect.

The second step in establishing the requirements consists in distributing the errors on the payload (measurement noise, scale factors, bias fluctuations, etc.) and on the satellite (thruster noise for the drag-free satellite and the attitude control, star sensor noise, position error, etc.). These errors have an impact either directly on the measured acceleration or on the *a posteriori* correction of the measurement.

The frequency distribution of the error has also been considered. Given that the measurement is performed at a well-known frequency fep, the stochastic noise can be partially rejected with the increase in the time integration Ti. The expression of the error budget is summarized as follows:

$$\left(\sqrt{\sum_{n_{ep}}S_{fep}^2}+\sqrt{\sum_{n'_{f'}}\left(\frac{S(f')}{R(f')}\right)^2}+\sqrt{\sum_{n''_i}\left(\frac{S(i\cdot fep)}{R(i\cdot fep)}\right)^2}\right)\oplus\sqrt{\sum_{n_r}\frac{S_r^2}{Ti}}<8.10^{-15}\,ms^{-2}$$

S_{fep} depicts each error source in phase at the EP frequency, which is the frequency of the Earth's gravitational field, modulated by the projection on the instrument axes and evaluated as 8 m/s^2 at 710 km altitude. $S(i.fep)$ are the error sources at the harmonic frequencies of fep, they are eliminated by a ratio $R(i.fep)$ depending on the harmonic. These ratios have been evaluated considering a single source at each harmonic frequency. $S(f')$ are the tone errors at frequencies different from multiples of the fep and eliminated by the ratio $R(f')$. All tone errors have been estimated and added together. Finally, the stochastic error S_r is eliminated by the integration time and summed quadratically with the tone errors.

The error distribution contains more than 80 sources for sine wave errors and 80 for stochastic sources. These are evaluated and validated during the manufacturing of the instrument, because they are deduced from one of the major functions of the instrument [81] or require specific experimentation to confirm the driven physical parameters [82], [83]. This error budget is derived to express more than 150 satellite and instrument major mission requirements, including the DC value of diving parameters that could be combined with the fep variations to generate a disturbance.

While the satellites were launched successively on April 25, the instrument was quickly switched on, on May 2nd, and the four masses were automatically electrostatically levitated, with the inertial sensors thereby providing their data. As from this date, the satellite quickly entered into a partial eclipse period that does not allow scientific measurements to be made, but only the operation assessment of the satellite and the payload. This is what is fruitfully being done. In order to achieve the MICROSCOPE mission objective, not only must the eventual violation measurement be performed, but also the Eötvös parameter accuracy obtained must be demonstrated.

Atomic interferometer

A new generation of complementary instruments, relying on the manipulation of matter waves through atom interferometry, appears nowadays as very promising for highly precise and accurate inertial measurements. Cold Atom interferometers have indeed proven on the ground to be very high performance sensors, with the development in recent decades of cold atom gravimeters [84], gravity gradiometers [85] and gyroscopes [86]. This promising technology has demonstrated performances that compete with other state-of-the-art gravimeters (superconducting or mass-spring devices) and is only expected to reach its full potential in space based applications. In such a micro-gravity environment, the interrogation time, and therefore the measurement scale factor, can be increased by orders of magnitude compared to ground-based sensors.

In a cold atom inertial sensor, the test mass is a gas of cold atoms obtained by laser cooling and trapping techniques. This cloud of cold

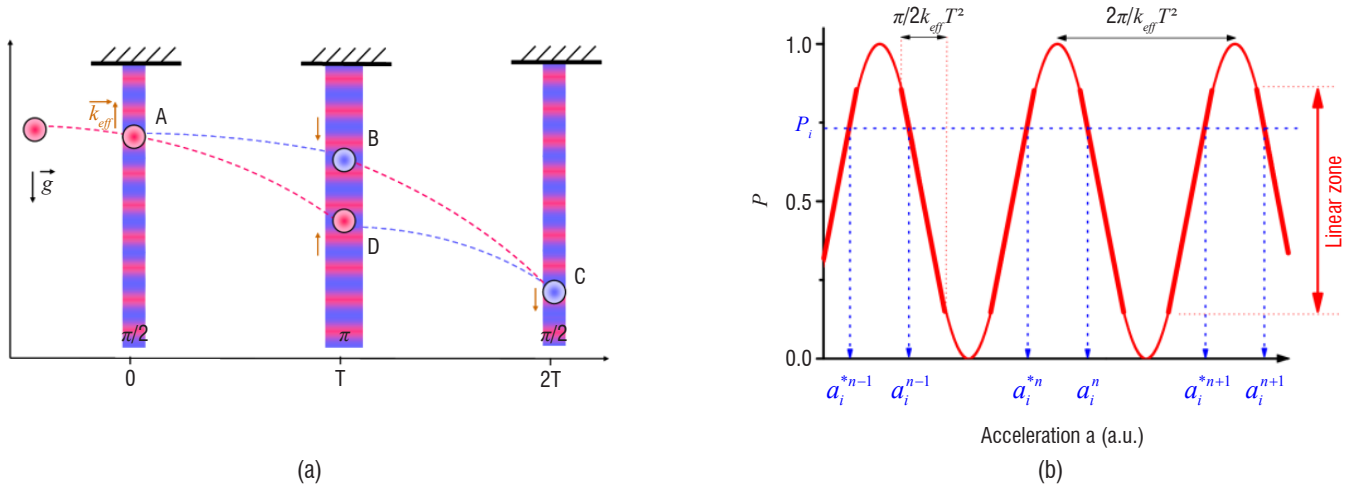

Figure 9 – (a) Mach-Zehnder type atom interferometer for gravity acceleration measurement. For such a gravimeter configuration, the three light pulses are separated only in time and not in space. (b) Output signal P_i of a cold atom accelerometer. One measurement P_i corresponds to several possible acceleration values a_i^n , a_i^{*n}.

atoms is released from a trap and, during free fall in a vacuum chamber, its displacement due to inertial forces is measured by an atom interferometry technique. Typically, an atom Mach-Zehnder type interferometer is made, consisting in a sequence of three equally spaced laser pulses allowing the atomic wave to be either equally split, deflected or re-combined (see Figure 9-a). The output signal from the instrument P depends sinusoidally on the phase of the interferometer (see Figure 9-b), which is proportional to the acceleration $\vec{a}$ of the atoms along the laser direction of propagation $\vec{k}_{eff}$: $P = \frac{1}{2} - \frac{1}{2}\cos(\vec{k}_{eff} \cdot \vec{a}\, T^2)$, where $\vec{k}_{eff}$ is the effective wave vector associated with the laser and T is the time between laser pulses. In the case where the acceleration to be measured is not subjected to large variations ($\Delta a << \frac{\pi}{2 k_{eff} T^2}$), it is possible thanks to a specific technique to identify the fringe index corresponding to the measurement and to retrieve the true acceleration value unambiguously. Otherwise, for large shot-to-shot acceleration variations ($\Delta a > \frac{\pi}{2k_{eff}T^2}$), the true acceleration value can no longer be recovered. Note that the measurement rate is typically of a few Hz for this kind of instrument. This ambiguity concerning the acceleration determination consequently reduces the shot-to-shot measurement range of cold atom sensors. With regard to this limitation, it is typical to associate a mechanical accelerometer to the cold atom instrument. This mechanical accelerometer allows the identification of the fringe index corresponding to the atomic acceleration measurement [87].

Following these measurement principles, cold atom interferometers have demonstrated on the ground performances comparable to those of other existing state-of-the-art technologies, especially concerning the development of gravimeters. At the present time, laboratory cold atom gravimeter performances have already exceed those of the conventional corner cube gravimeter, especially in terms of sensitivity, reaching 4.2 μGal/Hz$^{1/2}$ [88] (1 μGal = 10^{-8} m/s^2) and an accuracy of 5 μGal [89]. For most gravimeters, the sensitivity remains limited by the vibration noise background. Compared to conventional corner cube gravimeters, cold atom gravimeters can achieve a higher repetition rate, up to 300 Hz [90], and do not have movable mechanical parts. These features make cold atom gravimeters more suitable for on-board applications. In this context, in 2009 ONERA emphasized the on-board potential of this new generation of instruments, through the development of the GIRAFE cold atom gravimeter, designed especially for on-board applications. Despite the compactness of this instrument, the gravimeter has demonstrated a sensitivity of 42 μGal/Hz$^{1/2}$ and an accuracy of 25 μGal, close to that of state-of-the-art gravimeters [91]. Gravity measurements in an elevator were also conducted, leading to the determination of the Earth's gravity gradient along the vertical direction with a precision of 4 E (1 E = 0.1 μGal/m), and to first measurements of an atom gravimeter on a mobile platform.

Recently, ONERA has continued its research efforts in the field of on-board applications by developing a second generation cold atom gravimeter, GIRAFE 2, dedicated to boat gravity measurements (see Figure 10-a). In October 2015 and January 2016, ONERA in collaboration with SHOM tested and characterized this gravimeter when integrated on a gyro-stabilized platform during two marine campaigns, demonstrating successful results in terms of gravitational field mapping, even exceeding those obtained with the previous existing mechanical technology [92].

In the context of future Earth's gravity measurements in space, ONERA is also involved in a preliminary ESA study aimed at assessing the potential of combining the electrostatic technology and atom interferometry. These two technologies are clearly identified as very good candidates for future spatial missions dedicated to Earth observation. Each of these two types of instruments have their own assets which are, for electrostatic sensors, their demonstrated short term sensitivity and their maturity regarding the space environment and, for Atom Interferometers among others, the absolute nature of the measurement and therefore the lack of need for calibration processes. These two technologies seem in some aspects to be very complementary, and a hybrid sensor bringing together all of their assets could be the opportunity to take a big step in this context. ONERA, which has developed an expertise in each of these two technologies, is initiating a first experimental demonstration of a hybrid electrostatic-atomic instrument (see Figure 10-b) to begin the exploration of such an original sensor and to study its full potential for future gravity missions or aircraft applications.

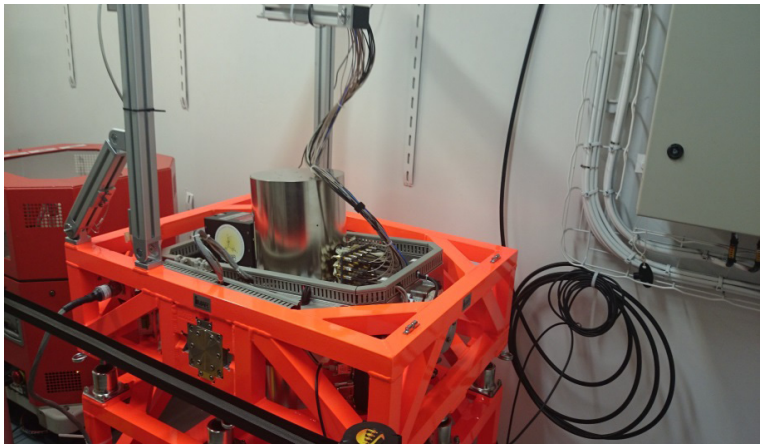

(a)

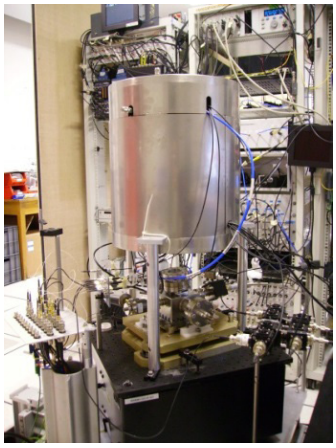

(b)

Figure 10 – (a) The cold atom gravimeter GIRAFE 2 with its gyrostabilized platform installed in the gravimetry room of the French ship Beautemps-Beaupré owned by SHOM. (b) The cold atom gravimeter GIRAFE coupled to an electrostatic accelerometer.

Mission and sensor perspectives

Concerning fundamental physics in space, it is clear that the MICROSCOPE mission must be followed by another similar space experiment with the same type of mission. If no EP violation is confirmed at the level of 10^{-15}, going beyond this accuracy must be sought and a cryogenic mission would help to gain another two orders of magnitude [93]. If a violation of the Equivalence Principle is detected, the violation must be confirmed and to analyzed, in particular according to different pairs of mass compositions. The same technology and concept can also be used for the detection of gravity waves in space as an inertial sensor. This is what is currently being demonstrated with promising results by the Lisa-Pathfinder payload of the eponym satellite for the e-Lisa mission [66], [94].

A reduced power and size sensor has been developed over the last years in our laboratory devoted to planetology. Interplanetary spacecraft require the mass to be reduced and the necessary power. This stand-alone instrument presents a cubic proof-mass, a volume of about 1 liter for 1 Watt consumption and its offsets along two of its sensitive axes are estimated and corrected in orbit. It can be used to map the gravitational field of celestial bodies, to measure residual atmosphere density or winds through satellite drag, or to perform long range Newton law tests during the transfer. This GAP sensor has been proposed to ESA in previous calls [95], [96].

Obviously, the common history of space geodesy and space accelerometers is not finished. Electrostatic accelerometers in space have been the corner stones of drastic improvements in the knowledge of the Earth's gravitational field: the GOCE mission (2009-2013) brought a strong improvement of the static part of the gravitational field, both in terms of space resolution (about 100 km) and in terms of accuracy, whereas since 2002 the GRACE mission has allowed the temporal evolution of gravity to be monitored, typically with a set of Stokes coefficients every month at a space resolution of about 300 km. These two kinds of concept will drive the needs of inertial sensors in space geodesy in the short and medium term. The results of the GRACE mission are so rich that there is a definite consensus from the community to continue this kind of monitoring with the least possible interruptions; following the example of space altimetry, the objective is to reconcile the robustness and the improvements by means of progressive evolutions. For example, GRACE Follow On (GFO), the successor of GRACE, will embark a new system based on laser interferometry to measure the relative velocity between the 2 craft, but this will be redundant with the microwave link already used on GRACE. GFO will use an accelerometer that is practically to the same as the GRACE instrument and with the same performances, at the 10^{-10} $ms^{-2}Hz^{-1/2}$ level. For the next step, when the reliability of the laser link is proved with an expected accuracy of 50 nanometers, the aim would be to have an accelerometer compatible with this level of performances, i.e., at the 10^{-11} $ms^{-2}Hz^{-1/2}$ level. This is the heart of the e.motion^2 mission proposed to ESA within the framework of the Explorer-9 program. There are also high hopes for cold atom accelerometers, but we do not currently know the exact limits of these sensors. If they prove to be competitive, a first step could be a mission embarking cold atom accelerometers together with electrostatic accelerometers.

The GOCE mission could also have a successor, but the context will not be the same as for GRACE. Continuity is not a main goal and the interest in a new gradiometric mission would be based on a substantial improvement of the performances. The need would be typically to go from the 10^{-12} $ms^{-2}Hz^{-1/2}$ level achieved for GOCE to 10^{-13} $ms^{-2}Hz^{-1/2}$. Since geodesists do not lack creativity, some of them have even thought about a hybrid concept associating gradiometric and SST techniques; this would involve 2 satellites with an inter-satellite link, with each satellite (or at least one of them) including one or several gradiometric arms.

However space accelerometers are not only useful to study the gravitational field. They are also very helpful to measure non-gravitational forces acting on the spacecraft. This has both a general and a specific interest. The general interest is to improve the quality of the dynamical model used to compute the trajectory, since gravitational forces are very tricky to compute; for example, errors of some tens of per cents are not rare in the prediction of the drag force due to the atmosphere. Thus, future geodetic missions such as the GRASP concept, which is aimed at the sub-centimeter level in terms of positioning, would be hardly achievable without an accelerometer [97]. The specific interest is to be able to perform in situ observations of the non-gravitational forces, in order to obtain information about their sources; this is the case of the atmosphere densities (the source of the drag force), which have been better modeled using the measurements of the STAR accelerometer on board the CHAMP satellite (2000-2010); this is also the case of radiative flux from the Earth (one of the sources of radiation pressure forces), which motivates mission concepts such as BIRAMIS, which is aimed at monitoring the Infra-Red and albedo radiations by means of accelerometric measurements [98]. This concept could be an option studied for the GRASP mission mentioned above.

Conclusion

The electrostatic levitation of a solid test mass is an old technology, but nevertheless a fruitful concept to design an ultra-sensitive space accelerometer. Squid detectors and superconductive magnetic levitation of the test mass have been proposed recently, but seem to have been forgotten because of their complexity for a space technology. In electrostatic sensors, the test mass motion is not only controlled with regard to the position but also with regard to the attitude, giving information on the angular acceleration of the satellite on which it is integrated. This the case of the GOCE satellite and would also be the case of the MICROSCOPE satellite, for which a fine attitude stability is required. The optimization of the accelerometer design requires mechanics and electronics experts, as well as physicists to deal with the disturbing forces acting on the test mass: this is an integrated team that Onera can offer for the described missions. The actual configuration of the sensor depends on the mission, the required full-scale range and the required resolution in a specific bandwidth. In order to improve the latter, it is now necessary to manage in orbit the test mass charging by the radiation flux through a solution other than the thin gold wire used and its disturbance damping: a photoelectric device could be the solution; it has already been implemented in the Lisa-Pathfinder inertial device configuration [99],[100],[101]. A gain by two orders of magnitude can be expected. The association with an atomic interferometer is also an avenue for the future, by taking advantage of the outstanding stability of the latter at low frequencies and the resolution of the electrostatic sensor at higher frequencies. What seemed to be old technology at the end of the last century now appears to be the key for future space missions at the beginning of the new century ■

Acknowledgment

The authors would like to thank all space team members who have contributed to the success of the mentioned space missions and, in particular, the MICROSCOPE mission. The development of the sensors has been party supported by ONERA and CNES.

References

[1] A. EINSTEIN - *The Meaning of General Relativity*. Princeton University Press, New Jersey, 5th edition, 1956.
[2] M. E. PESKIN - *Theoretical Summary Lecture for the Higgs Huning 2012*. arXiv:1208.5152v2 [hep-ph.] 8 Sep 2012.
[3] B. P. ABBOTT *et al.* - *Observation of Gravitational Waves from Binary Black Hole Merger*. PRL 116, 061102, 2016.
[4] CHAMP - http://op.gfz-potsdam.de/champ/
[5] GRACE - http://science.nasa.gov/missions/grace/
[6] GOCE - http://www.esa.int/Our_Activities/Observing_the_Earth/GOCE/
[7] A. LAWRENCE - "*Modern Inertial Technology: Navigation, Guidance and Control*". Springer, second edition, 1998.
[8] R. E. HOPKINS, F. K. MUELLER, W. HAEUSSERMANN - *The Pendulous Integrating Gyroscope Accelerometer (PIGA) from the V-2 to Trident D5, the Strategic Instrument of Choice*. Navigation, and Control Conference & Exhibit, 6-9 August 2001 Montreal, Canada, 2001.
[9] S.A. FOOTE, D. B. GRINDELAND - *Model QA3000 Q-Flex Accelerometer High Performance Test Results*. IEEE Aerospace and Electronic Systems Magazine, 1992, Volume: 7, Issue: 6, p. 59-67, DOI: 10.1109/62.145120.
[10] H. C. HAYES - *Method and Apparatus for Determining the Force of Gravity*. US Patent n° 1,995,305 filed Oct. 1928, 1935.
[11] G. MAMON - *A Traverse Gravimeter for the Lunar Surface*. IEEE Transactions on Geoscience Electronics, Vol. GE-10, n° 1, p. 64-72, 1972.
[12] J. KRITZ - *Accelerometer*. US Patent n° 2,984,111, filed June 1959, 1961.
[13] J. KRITZ *et al.* - *Accelerometer and Parts Therefor*. US Patent n° 3,190,129, filed July 1961, 1965.
[14] F.A NORRIS *et al.* - *Piezoelectric Force Transducer*. US Patent n° 3,479,536, filed March 1967, 1969.
[15] L. WEISBORD - *Single Beam Force Transducer with Integral Mounting Isolation*. US Patent n° 3,470,400, filed Dec. 1967, 1969.
[16] J. M. PAROS *et al.* - *Longitudinal Isolation System for Flexurally Vibrating Force Transducers*. US Patent n° 4,321,500, filed Dec. 1979, 1982.
[17] W. C. ALBERT *et al.* - *Non-Prismal Beam Resonator*. US Patent n° 4,445,065, filed Sep. 1981, 1984.
[18] W. C. ALBERT *et al.* - *Vibrating Beam Force Transducer with Angled Isolator Springs*, US Patent n° 4,658,174, filed Mar. 1986, 1987.
[19] H. FIMA & D. JANIAUD - *Vibrating String Resonator*. US Patent n° 4,710,668, filed Dec. 1985, 1987.
[20] E. NISSE - *Miniature Quartz Resonator Force Transducer*. US Patent n° 4,215,570, filed Apr. 1979, 1980.
[21] R. G. KIRMAN *et al.* - *Force sensors*. US Patent n° 4,594,898, filed Jun. 1984, 1986.
[22] B. L. NORLING *et al.* - *Accelerometer with Isolator for Common Mode Inputs*. US Patent n° 4,766,768, filed Oct. 1987, published Aug. 1988.
[23] https://aero1.honeywell.com/inertsensor/rba500.shtml
[24] K.E. PETERSEN - *Silicon as Mechanical Material*. Proceeding of the IEEE, Volume:70, Issue:5, Pages:420-457, 1982.
[25] R. T. HOWE *et al.* - *Resonant Accelerometer*. US Patent n° 4,805,456, filed May 1987, 1989.
[26] T. V. ROSZHART - "*Silicon Micromachined Accelerometer*", US Patent n° 4,945,765, filed Aug. 1988, published Aug. 1990.
[27] D. JANIAUD *et al.* - *Accelerometric Sensor with Flectional Vibratory Beam*. US Patent n° 5,170,665, filed Aug. 1990, 1992.
[28] W. C. ALBERT - *Monolythic Resonator Vibrating Beam Accelerometer*. US Patent n° 4,804,875, filed Sep. 1982, 1989
[29] O. LE TRAON *et al.* - *The VIA Vibrating Beam Accelerometer: Concept and Performances*. Proceedings of the Position, Location and Navigation Symposium, Palm springs, 1998.
[30] G.R. NEWELL *et al.* - *Accelerometer and Method of Manufacture*. US Patent n° 5,5755,978, filed Dec. 1996, 1998.
[31] R. JAFFE, T. ASHTON, A. MADNI - *Advances in Ruggedized Quartz MEMS Inertial Measurement Units*. IEEE/ION PLANS, Coronado, CA, April 2006.

[32] T. V. ROSZHART, H. JERMAN, J. DRAKE, C. DE COTIIS - *An Inertial-Grade Micormachined Vibrating Beam Accelerometer*. Transducers'95 & EuroSensors IX, 1995.

[33] R. LEONARDSON, S. FOOTE - *SiMMA Accelerometer for Inertial Guidance and Navigation*. Position Location and Navigation symposium IEEE, p. 152-160, Palm Spring, USA, 1998.

[34] M. HELSEL, G. GASSNER, M. ROBINSON, J. WOODRUFF - *A Navigation Grade Micro-Machined Silicon Accelerometer*. Position Location and Navigation Symposium, 1994, IEEE 11-15, p. 51-58, 1994.

[35] R. HOPKINS *et al.* - *The Silicon Oscillating Accelerometer: A High-Performance MEMS Accelerometer for Precision Navigation and Strategis Guidance Applications*. ION 61st Annual Meeting, Cambridge, MA, June 2005.

[36] S. F. BECKA, M. NOVACK, S. SLIVINSKY, C.PAUL - *A High Reliability Solid State Accelerometer for Balistic Missile Inertial Guidance*. AIAA Guidance, Navigation and Control Conference, Aug. 2008.

[37] O. LEFORT, S. JAUD, R. QUER, A. MILESI - *Inertial Grade Silicon Vibrating Beam Accelerometer*. Symposium Gyro Technology, Sept. 2012.

[38] O. LE TRAON, D. JANIAUD, B. LECORRE, S. MULLER, M. PERNICE - *Mechanical Decoupling Device for Monolithic Differential Vibrating Sensor*. US patent n° 7448268 B, 2008

[39] J. LECLERC - *MEMS for Aerospace Navigation*. Aerospace and Electronic Systems Magazine , IEEE, Volume: 22, Issue: 10, p. 31-36, 2007.

[40] A. JEANROY, P. FEATONBY, J-M. CARON - *Low-Cost Miniature and Accurate IMU with Vibrating Sensors for Tactical Applications*. Symposium Gyro Technology 2003, Stuttgart.

[41] T. LORET, G. HARDY, C. VALLÉE, V. DEMUTRECY, T. KERRIEN, S. COCHAIN, D. BOUTOILLE, R. TAÏBI, R. BLONDEAU - 2014 DGON Inertial Sensors and Systems (ISS).

[42] O. LE TRAON, D. JANIAUD, S. MULLER - *Monolithic acceleration transduce*. US patent n° 5962786 A, 1999.

[43] R. LEVY, O. LE TRAON, S. MASSON, O. DUCLOUX, D. JANIAUD, J. GUÉRARD, V. GAUDINEAU, C. CHARTIER - *An Integrated Resonator-Based Thermal Compensation for Vibrating Beam Accelerometers*. Sensors, IEEE 978-1-4877-1787, 2012.

[44] R. LEVY, D. JANIAUD, J. GUERARD, R. TAÏBI, O. LE TRAON - *A 50 Nano-g Resolution Quartz Vibrating Beam Accelerometer*. 2014 International Symposium on Inertial Sensors and Systems (ISISS).

[45] A. PEREZ, A. M. SHKEL - *Design and Demonstration of a Bulk Micromachined Fabry–Pérot μg – Resolution Accelerometer*.

[46] C.-H. LIU, T. W. KENNY - *A High-Precision, Wide-Bandwidth Micromachined Tunneling Accelerometer*. 1057-7157, IEEE, 2001.

[47] J. LI *et al.* - *On-Orbit Performance of Gravity Probe B Drag-Free Translation Control and Orbit Determination*. Advances in Space Research, 40, 1-10, 2007.

[48] P. TOUBOUL, G. MÉTRIS, V. LEBAT, A. ROBERT - *The MICROSCOPE Experiment, Ready for the In-Orbit Test of the Equivalence Principle*. Class. Quantum Grav. 29, 18, 2012.

[49] E. DOORNBOS *et al.* - *Neutral density and crosswind determination from arbitrarily multiaxis accelerometers on satellite*. Journal of spacecraft and rockets, 47, 4, 2001.

[50] B. D. TAPLEY *et al.* - *GRACE Measurements of Mass Variability in the Earth System*. 305, 5883, p. 503-505, 2004.

[51] E. CANUTO, L. MASSOTTI - *All-Propulsion Design of the Drag-Free and Attitude Control of the European Satellite GOCE*. Acta astronautica, 64,2-3, p. 325-344, 2009.

[52] H. NYQUIST - *Thermal Agitation of Electric Charge in Conductors*. Phys. Rev. 32,110,1928.

[53] C.W. MC COMBIE - *Flucutation Theory in Physical Measurements*. Reports on Progress In Phys., 16, 266, 1953.

[54] F. GRASSIA, J.-M. COURTY, S. REYNAUD, P. TOUBOUL - *Quantum Theory of Fluctuations in a Cold Damped Accelerometer*. The European Phys. Journal D 8, 101-110, 2000.

[55] S. T. RUGGIERO, D. A. RUDMAN - *Superconducting Devices*. Academic Press Inc., 1990.

[56] R KLEINER, D. KOELLE, F. LUDWIG, J. CLARKE - *Superconducting Quantum Interference Devices: State of the Art and Application*. IEEE 92, 10, 2004.

[57] J. CLARKE, A. I. BRAGINSKI - *The SQUID Handbook*. Wiley-VCH Verlag mbH & Co.LGaA, 2006.

[58] H. J. PAIK, J-P. BLASER, S. VITALE - *Principle of the STEP Accelerometer Design*. Adv. Space Res., 32, 7, p. 1325-1333, 2003.

[59] J. OVERDUIN, F. EVERITT, P. WORDEN, J. MESTER - *STEP and Fundamental Physics*. Class Quantum Grav. 29, 18, 2012.

[60] H. A. CHAN, H. Y. PAIK - *Superconducting Gravity Gradiometer for Sensitive Measurements*. Physical Review. I Theory, 35, 12, 1987.

[61] H. A. CHAN, M. V. MOODY, H. Y. PAIK - *Superconducting Gravity Gradiometer for Sensitive Measurements.* II Experiment, Physical Review, 35, 12, 1987.

[62] http://www.nasa.gov/mission_pages/gpb/

[63] S. BUCHMAN, J. P. TURNEAURE - *The Effects of Patch-Potentials on The Gravity Probe B Gyroscopes*. Rev. Sci; Instrument, 82, 074502, 2011.

[64] P. TOUBOUL, B. FOULON, E. WILLIEMENOT - *Electrostatic Space Accelerometers for Present and Future Missions*. Acta Astrautica, 45, 10, p 605-617, 1999.

[65] P. TOUBOUL, B. FOULON, M. RODRIGUES, J.-P. MARQUE - *In Orbit Nano-g Measurements, Lessons for Future Space Missions.* Aerospace Science and Technology 8, p 431-441, 2004.

[66] http://sci.esa.int/lisa-pathfinder/

[67] P. MCNAMARA, S. VITAL, K. DANZMANN - *LISA Pathfinder*. Class. Quantum Grav., 25, 114034, 2008.

[68] V. JOSSELIN, M. RODRIGUES, P. TOUBOUL - *Inertial Sensor Concept for the Gravity Wave Missions*. Acta Astronautica 49, 2, p.95-103, 2001.

[69] E. WILLEMENOT, P. TOUBOUL - *On-Ground Investigation of Space Accelerometers Noise with an Electrostatic Torsion Pendulum*. Rev. Sci. Instrum. 71, 302 (2000); doi: 10.1063/1.1150197.

[70] A. CAVALLERI *et al.* - *Direct Force Measurements for Testing the Lisa Pathfinder Gravitational Reference Sensor*. Class. Quantum Grav. 26 (2009) 094012.

[71] J.-P. MARQUE, B. CHRISTOPHE, B. FOULON - *Accelerometers of the GOCE Mission: Return of Experience from One Year of In-Orbit*. Proc. 'ESA Living Planet Symposium', Bergen, Norway 28 June - 2 July 2010 (ESA SP-686, December 2010).

[72] B. CHRISTOPHE, D. BOULANGER, B. FOULON, P.-A. HUYNH, V. LEBAT, F. LIORZOU, E. PERROT - *A New Generation of Ultra-Sensitive Electrostatic Accelerometers for GRACE Follow-On and Towards the Next Generation Gravity Missions*. Acta Astronautica 117 (2015) 1-7.

[73] J. FLURY, S. BETTADPUR, B. D. TAPLEY - *Precise Accelerometry Onboard the GRACE Gravity Field Satellite Mission*. Advances in Space Research 42 (2008) 1414-1423.

[74] CHRISTOPHE, B., J. MARQUE, B. FOULON - *In-Orbit Data Verification of the Accelerometers of the ESA GOCE Mission*. SF2A-2010: Proceedings of the Annual meeting of the French Society of Astronomy and Astrophysics. Vol. 1, 2010.

[75] G. RUSSANO - *A Torsion Pendulum Ground Test of the LISA Pathfinder Free-Fall Mode.* Doctoral Thesis, University of Trento, 2015.

[76] M. BASSAN *et al.* - *Approaching Free Fall on Two Degrees of Freedom: Simultaneous Measurement of Residual Force and Torque on a Double Torsion Pendulum*. PRL 116, 051104, 2016.

[77] Drop Tower Operation and Service Company - *ZARM Drop Tower Bremen User Manual.* ZARM FABmbH, Bremen, 2012.

[78] H. SELIG *et al.* - *Drop Tower Microgravity Improvement Towards the Nano-g Level for the MICROSCOPE Payload Tests*. Microgravity Sci. Technol. 22, 2010.

[79] A. EINSTEIN - *Die Grundlage der allgemeinen Relativitätstheorie*. Annalen der Physik 354 (7), 769-822, 1916.

[80] P. TOUBOUL - *The MICROSCOPE Mission and its Uncertainty Analysis*. Space Sci Rev 148: 455-474, 2009.

[81] V. JOSSELIN, P. TOUBOUL, R. KIELBASA - *Capacitive Position Sensing for Space Accelerometers Applications*. Sensors and Actuator, 78, 2-3, p 92-98, 1999.

[82] E. WILLEMENOT, P. TOUBOUL - *Electrostatically Suspended Torsion Pendulum*. Rev. Scien. Instr. 71, 310, 2000.

[83] E. WILLEMENOT, P. TOUBOUL - *On-Ground Investigation of Space Accelerometers Noise with an Electrostatic Torsion Pendulum*. Rev. Scien. Instr. 71, 302, 2000.

[84] A. PETERS, K. Y. CHUNG, S. CHU - *High-Precision Gravity Measurements Using Atom Interferometry.* Metrologia 38, 25, 2001.

[85] J. M. MCGUIRK, G. T. FOSTER, J. B. FIXLER, M. J. SNADDEN, M. A. KASEVICH - *Sensitive Absolute-Gravity Gradiometry Using Atom Interferometry*. Phys. Rev. A 65, 033608, 2002.

[86] T. L. GUSTAVSON, P. BOUYER, M. A. KASEVICH - *Precision Rotation Measurements with an Atom Interferometer Gyroscope*. Phys. Rev. Lett. 78, 2046, 1997.

[87] R. GEIGER, V. MÉNORET, G. STERN, N. ZAHZAM, P. CHEINET, B. BATTELIER, A. VILLING, F. MORON, M. LOURS, Y. BIDEL, A. BRESSON, A. LANDRAGIN, P. BOUYER - *Detecting Inertial Effects with Airborne Matter-Wave Interferometry*. Nature Communications 2, 474, 2011.

[88] Z.-K. HU, B.-L. SUN, X.-C. DUAN, M.-K. ZHOU, L.-L. CHEN, S. ZHAN, Q.-Z. ZHANG, J. LUO - *Demonstration of an Ultrahigh-Sensitivity Atom-Interferometry Absolute Gravimeter.* Phys. Rev. A 88, 043610, 2013.

[89] A. LOUCHET-CHAUVET, T. FARAH, Q. BODART, A. CLAIRON, A. LANDRAGIN, S. MERLET, F. PEREIRA DOS SANTOS - *The Influence of Transverse Motion within an Atomic Gravimeter*. New J. Phys. 13, 065025, 2011.

[90] H. J. MCGUINNESS, A. V. RAKHOLIA, G. W. BIEDERMANN - *High Data-Rate Atom Interferometer for Measuring Acceleration*. Appl. Phys. Lett. 100, 011106, 2012.

[91] Y. BIDEL, O. CARRAZ, R. CHARRIÈRE, M. CADORET, N. ZAHZAM, A. BRESSON - *Compact Cold Atom Gravimeter for Field Applications*. Appl. Phys. Lett. 102 , 144107, 2013.

[92] http://www.onera.fr/fr/actualites/cartographie-marine-haute-precision-pesanteur-atomes-froids

[93] P. TOUBOUL, M. RODRIGUES, E. WILLEMENOT, A. BERNARD - *Electrostatic Accelerometers for the Equivalence Principle Test in Space*. Class. Quantum Grav. 13, A67-A78, 1996.

[94] https://www.elisascience.org/

[95] B. CHRISTOPHE *et al.* - *Odyssey: A Solar System Mission*. Exp Astron 23:529-547, 2009.

[96] B. CHRISTOPHE *et al.* - *OSS (Outer Solar System): A Fundamental and Planetary Physics Mission to Neptune, Triton and the Kuiper Belt*. Exp Astron 34:203-242, 2012.

[97] Y. BAR-SEVER, B. HAINES, W. BERTIGER, S. DESAI, S. WU - *Geodetic Reference Antenna in Space (GRASP) – A Mission to Enhance Space-Based Geodesy*. ilrs.gsfc.nasa.gov/docs/GRASP_COSPAR_paper.pdf

[98] G. DUCHOSSOIS - *Potential European Climatological Satellite Missions: SEOCS and BIRAMIS*. Acta Astronautica Vol 7, 385-399, 1980.

[99] T. SUMNER *et al.* - *LISA and LISA Pathfinder Charging* . Class. and Quant. Gravity, 26,094006, 2009.

[100] D. HOLLINGTON – thesis: *The Charge Management System for LISA and LISA Pathfinder*. High Energy Physics Group, Department of Physics, Imperial College London, 2011.

[101] D. HOLLINGTON, J. T. BAIRD, T. J. SUMNER, P. J. WASS - *Characterising and Testing Deep UV LEDs for Use in Space Applications*, Class. and Quant. Gravity vol.32, N°23, 2015.

Acronyms

AVAS	(Accéléromètre Vibrant pour Applications Spatiales)
CERN	(Conseil Européen pour la Recherche Nucléaire)
CHAMP	(CHAllenging Minisatellite Payload)
eLISA	(European Laser Interferometer Space Antenna)
ESA	(European Space Agency)
FSR	(Full Scale Range)
GAP	(Gravity Accelerometer Package)
GPB	(Gravity Probe B)
GOCE	(Gravity field and steady-state Ocean Circulation Explorer)
GRACE	(Gravity Recovery And Climate Experiment)
GRASP	(Geodetic Reference Antenna in SPace)
MEMS	(Micro-Electro-Mechanical System)
MICROSCOPE	(MICRO- Satellite pour l'Observation du Principe d'Equivalence)
NASA	(National Aeronautics and Space Administration)
PIGA	(Pendulous Integrating Gyroscope Accelerometer)

SQUID	(Superconducting Quantum Interference Device)
SST	(Standard Star Tracker)
STAR	(Space Three-Axis Accelerometer for Research)
VBA	(Vibrating Beam Accelerometer)
VSA	(Vibrating String Accelerometer)
ZARM	(Zentrum für Angewandte Raumfahrttechnologie und Mikrogravitation)

AUTHORS

Pierre Touboul is since 2010 Scientific Director of the Physics Branch at the French Aerospace Lab, ONERA. He is recipient in 2004 of the Award in Physics, "Prix Montgolfier" and of the "Grand Prix Marcel Dassault" from French Science Academy. He awards in 2010 the annual "Grand Prix" from French Air and Space Academy for the success of the space accelerometers on board the international CHAMP, GRACE and GOCE missions. His major scientific contribution, as instrumentalist, concerns space accelerometry, geodesy and fundamental physics space missions, with major contributions to the scientific payloads of already four successful missions. He is presently Prime Investigator of the Cnes-ESA MICOSCOPE mission, co-author of patents, more than seventy peer-reviewed publications, over one hundred Onera reports and international conference papers.

Gilles Metris is Astronomer at laboratory Géoazur of Nice University, Côte d'Azur Observatory and CNRS. Its themes of research concern celestial mechanics including modeling orbital dynamics of spacecraft and applications to the knowledge of environment in which they move: gravity field of the Earth, small non-gravitationnal forces, tests of gravitation in weak field… Gilles Metris is also Co-PI of the MICROSCOPE mission.

Hanns Sélig. After his degree in physics and astrophysics at the University of Hamburg and some work at the Observatory Hamburg-Bergedorf and DESY, he moved to ZARM (University of Bremen) where he started to work on MICROSCOPE in 2001.

Olivier Le Traon obtained an Engineering degree from INSA Lyon (*Institut National des Sciences Appliquées*) in 1986 and a master degree in Solid Mechanics and Modeling. He joined the Physics and Instrumentation Department of ONERA (the French Aerospace Lab) in 1991. His research interests concern micro and nanotechnologies and resonators, in particular Inertial Vibrating MEMS (Vibrating Beam Accelerometers and Coriolis Vibrating Gyros). Since 2012, he is Deputy Director of Physics and Instrumentation Department at ONERA.

Alexandre Bresson. Engineer graduated from SupOptique (France), PhD in Physics (2000), he is currently Research Scientist at ONERA, in charge of atom inertial sensor development. He Heads the research unit SLM (Laser Sources and Metrology) at DMPH (Physics and Instrumentation department).

N. Zahzam was born in 1979. In 2005, he obtained his Ph. D degree devoted to the study of Bose-Einstein condensation, cold atoms and molecules trapping. Since 2006, he has worked at ONERA in the field of cold atom interferometry

Bruno Christophe graduated from ISAE/SupAéro Engineer school in 1990. He joined ONERA in the Syntheses Study Direction in 1990. In 2000, he joined the Physics and Instrumentation Department at ONERA for GOCE accelerometer development, as Technical Manager. Since 2011, he is head of Instrumentation and Aerospace Equipment, involved in the space accelerometer development and project manager of GRACE-FO accelerometer. He is member of CNES advisory group for fundamental physics since 2011.

Manuel Rodrigues is research engineer in physics from the *Ecole Supérieure de Physique et de Chimie Industrielles de la ville de Paris*. In ONERA since 1991, he was first involved in test bench development for thin film sensor for aeronautics and space equipment, and then became MICROSCOPE Project manager.